
MTL-KD: Multi-Task Learning Via Knowledge Distillation for Generalizable Neural Vehicle Routing Solver

Yuepeng Zheng¹ Fu Luo¹, Zhenkun Wang³, Yaxin Wu⁴, Yu Zhou^{1*}

¹ College of Computer Science and Software Engineering,
Shenzhen University, Shenzhen, China

² Guangdong Provincial Key Laboratory of Fully Actuated System Control Theory and Technology,
School of Automation and Intelligent Manufacturing,
Southern University of Science and Technology, Shenzhen, China

³ Guangdong Provincial Key Laboratory of Fully Actuated System Control Theory and Technology,
School of Automation and Intelligent Manufacturing,
Southern University of Science and Technology, Shenzhen, China

⁴ Eindhoven Artificial Intelligence Systems Institute
& Department of Industrial Engineering and Innovation Sciences,
Eindhoven University of Technology, Eindhoven, The Netherlands

2019271024@email.szu.edu.cn, luof2023@mail.sustech.edu.cn
wangzhenkun90@gmail.com, y.wu2@tue.nl, zhousy_1022@126.com

Abstract

Multi-Task Learning (MTL) in Neural Combinatorial Optimization (NCO) is a promising approach to train a unified model capable of solving multiple Vehicle Routing Problem (VRP) variants. However, existing Reinforcement Learning (RL)-based multi-task methods can only train light decoder models on small-scale problems, exhibiting limited generalization ability when solving large-scale problems. To overcome this limitation, this work introduces a novel multi-task learning method driven by knowledge distillation (MTL-KD), which enables the efficient training of heavy decoder models with strong generalization ability. The proposed MTL-KD method transfers policy knowledge from multiple distinct RL-based single-task models to a single heavy decoder model, facilitating label-free training and effectively improving the model's generalization ability across diverse tasks. In addition, we introduce a flexible inference strategy termed Random Reordering Re-Construction (R3C), which is specifically adapted for diverse VRP tasks and further boosts the performance of the multi-task model. Experimental results on 6 seen and 10 unseen VRP variants with up to 1000 nodes indicate that our proposed method consistently achieves superior performance on both uniform and real-world benchmarks, demonstrating robust generalization abilities.

1 Introduction

The Vehicle Routing Problem stands as a recognized classical challenge within the field of combinatorial optimization. Due to its widespread applicability across numerous real-world scenarios [1–3], including logistics distribution, traffic scheduling, and emergency response, the VRP has consistently been a subject of intense research interest. However, traditional optimization algorithms [4–6] often necessitate intricate domain-specific knowledge for their design and exhibit limitations in efficiency when applied to large-scale instances, thereby hindering their scalability in practical applications.

*Corresponding author

In recent years, Neural Solvers [7–10] have demonstrated significant potential in tackling VRPs. These models offer high computational efficiency and reduced reliance on domain-specific knowledge, achieving competitive performance with traditional algorithms. However, the inherent design of these single-task models significantly restricts their versatility in handling diverse problem instances. The necessity to retrain the model even for slightly different problem settings severely limits their practical utility.

The diverse nature of VRPs in the real world has spurred recent research efforts to develop unified models capable of solving multiple VRP variants and exhibiting good generalization on unseen tasks[11–13]. Currently, the majority of unified models for VRP variants adopt a heavy encoder-light decoder (HELD) architecture. These models have relatively low computational costs and can be directly trained using RL, demonstrating excellent performance on small-scale problems. However, their generalization ability significantly deteriorates when dealing with large-scale instances, primarily because the light decoder struggles to extract sufficient information from the high-density and complex node embeddings[14]. Furthermore, training them on large-scale instances also presents the challenge of excessively large gradient information, collectively leading to the inadequacy of existing VRP variant models in handling large-scale problems.

On the other hand, the light encoder-heavy decoder[15–17] architecture has demonstrated excellent generalization capabilities on large-scale problems. Its iterative decoding process, where the heavy decoder continuously re-evaluates the relationships between the remaining nodes, coupled with the dynamic change in the number of nodes, contributes to the strong scale generalization performance of this architecture. To achieve scale generalization within a multi-task unified model, we aim to leverage the heavy decoder architecture. However, the substantial memory and computational demands inherent in heavy decoders render direct RL impractical; they typically employ supervised learning, which necessitates extensive labeled data, a demand further amplified by multi-task training. While SIT[17] employs a self-improved Training method using operations like local reconstruction [15] to refine model-generated solutions as training labels, this suffers from the generation of numerous low-quality labels during early and mid-training, leading to a protracted process and an increased training burden due to time-consuming pseudo-label generation. We provide a comprehensive literature review on autoregressive neural solvers and multi-task neural solvers for VRPs in Appendix A.

To address the limitations of existing supervised training methods for heavy decoders, we introduce knowledge distillation as a novel training paradigm for the heavy decoder model, thereby circumventing the need for extensive label generation. We employ easily RL-trained HELD teacher models as supervision to train our multi-task heavy decoder model, thus achieving label-free training for the heavy decoder. The heavy decoder model trained with this method demonstrates strong generalization performance across both scales and tasks. Furthermore, during inference, we propose a general Random Reordering Reconstruction strategy for various VRP variants. By randomly reordering the external order of subtours, R3C significantly enhances solution sampling diversity, mitigates the risk of getting trapped in local optima, and further improves performance. Our contributions are summarized as follows: 1) We achieve efficient label-free training of heavy decoder models for multi-task VRPs through knowledge distillation. 2) We propose a novel R3C strategy to further enhance the performance of the multi-task model. 3) The MTL-KD model demonstrates excellent performance on seen training tasks, unseen tasks, and real-world datasets, exhibiting good scale generalization ability and significantly outperforming existing multi-task VRP models.

2 Preliminaries

Capacitated Vehicle Routing Problem and Its Variants The Capacitated Vehicle Routing Problem (CVRP) is typically defined as follows: Given a central depot v_0 and N customer nodes v_1 to v_n , all interconnected with distances e_{ij} . Each customer i has a demand d_i , and all vehicles depart from the depot, serve customers, and return to the depot. Each vehicle has a capacity C , satisfying $C > d_i$. All customers must be visited exactly once, and the total load of the vehicle during its route must not exceed its capacity. The objective of CVRP is to minimize the total travel distance of all vehicles.

By introducing additional constraints, CVRP can be extended into various variants. The four types of additional constraints studied in this paper include: **(1) Open Route (O):** Vehicles are not required to return to the depot after completing their service. **(2) Time Windows (TW):** Each node i has a service time window $[s_i, l_i]$, within which vehicles must arrive at the customer (early arrivals require

waiting until the earliest service start time). **(3) Backhaul (B):** Customer demands can be positive (linehauls) or negative (backhauls), and there is no restriction on the sequence of visiting linehauls and backhauls customers. **(4) Duration Limit (L):** The total travel distance of each vehicle must not exceed a predefined threshold L . Combining these constraints with CVRP can form 16 different VRP variants, with specific details provided in Appendix B.

Solution Construction Process by Neural Solver Constructive neural solvers [7, 8, 15] typically employ an encoder-decoder architecture and construct solutions in an autoregressive manner. For a given VRP instance $\mathcal{G} = (V, E)$, where V denotes the set of nodes, including node features such as demand, and E represents the set of edges, often formed by a distance matrix. The encoder is used to extract node information and generate embedding vectors for each node, while the decoder constructs the next node based on the current partial solution state s_{t-1} . The decoder is subject to node constraints during the construction process to avoid generating infeasible solutions. The entire solving process can be represented as:

$$\pi_\theta(\tau|\mathcal{G}) = \prod_{t=1}^{\ell} \pi_\theta(a_t|s_t, \mathcal{G}),$$

where τ is the complete solution, a_t is the action (node) selected at time step t , and ℓ is the total number of actions. The decoder continuously constructs nodes until all nodes have been visited, forming a complete solution. Through training, the model learns how to effectively select the next node based on the current partial solution, thereby optimizing the quality of the entire solution.

Knowledge distillation Knowledge Distillation[18] is a model compression and knowledge transfer technique aimed at transferring the knowledge learned by a high-performing, pre-trained teacher model to a smaller student model. The core idea is to achieve this transfer by minimizing the discrepancy between the outputs of the teacher and student models. The student model’s training loss typically includes a distillation loss (L_{KD}) that measures the difference between the student’s predictions and the teacher’s soft targets, generally the KL divergence $L_{KD} = \text{KL}(\pi_T || \pi_S)$. Additionally, depending on the specific task requirements, an original task loss (L_{Task}) can optionally be included, and the total loss (L) for the student model can be expressed as:

$$L = \alpha L_{KD} + (1 - \alpha) L_{Task}$$

where (α) is a weight parameter. In the field of Neural Combinatorial Optimization, knowledge distillation has been used to achieve model lightweighting and can improve the generalization ability of models on unseen problems to a certain extent[19–22].

3 Multi-Task Learning Via Knowledge Distillation

In this section, we propose a multi-task learning framework via knowledge distillation to address the challenge of applying heavy decoder models in the multi-task domain due to their reliance on large amounts of labeled data. The proposed framework effectively enhances the model’s generalization capabilities across different tasks and scales.

3.1 Framework Overview

Our proposed multi-task training framework via knowledge distillation aims to enhance the model’s generalization capabilities across different tasks and scales. As depicted in Figure 1, the framework first categorizes VRP variants into seen and unseen tasks for model training. Given N seen tasks, we first pre-train N individual teacher models employing a Light Encoder-Heavy Decoder architecture[15]. Subsequently, we construct a multi-task heavy decoder student model and train it using knowledge distillation, leveraging the output distributions of the teacher models as supervision signals.

3.2 Teacher Model Training

For each seen VRP variant task, we first generate the corresponding instance data. Then, we independently train a teacher model for each task, which adopts the POMO[8] structure and serves as

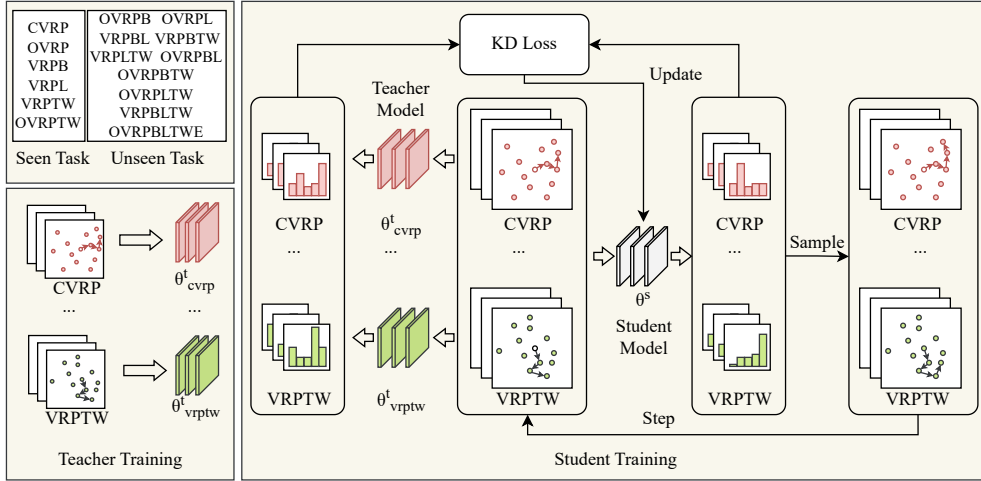


Figure 1: Framework for Multi-Task Training via Knowledge Distillation. Top-left: seen and unseen tasks. Bottom-left: Independent training of teacher models. Right: Student model distillation via teacher output distributions.

a policy network. We optimize the parameters of the teacher models using the policy gradient method in RL, with the objective of maximizing the reward (negative tour length). The loss function[23] can be expressed as:

$$L(\theta^T) = -\mathbb{E}_{\tau \sim \pi_{\theta^T}(\cdot | \mathcal{G})}[(r(\tau) - b^T(\mathcal{G})) \log \pi_{\theta^T}(\tau | \mathcal{G})]$$

where $b^T(\mathcal{G})$ is the baseline (average reward of multi-start trajectories for the instance), π_{θ^T} is the teacher model’s policy distribution, θ^T represents the parameters, and r is the reward.

3.3 Student Model Training

During the student model training phase, we construct a multi-task heavy decoder model. In each training batch, we simultaneously generate instance data for the N seen problem types and feed them into the student model for processing. At each decoding step t , the student model outputs a predicted probability distribution over the next nodes $\pi_{\theta^S}(a_t | s_t, \mathcal{G})$, encompassing the probability distributions for the N problem types. Concurrently, we input each problem instance to its corresponding pre-trained teacher model to obtain the teacher model’s probability distribution $\pi_{\theta^T_n}(a_t | s_t, \mathcal{G})$ under the same state s_t . We calculate the Kullback-Leibler divergence between the student model’s output probability distribution and the corresponding teacher model’s output probability distribution as the knowledge distillation loss $L_{KD}^{(t)}$:

$$L_{KD}^{(t)} = \sum_{n=1}^N \text{KL}(\pi_{\theta^T_n}(a_t | s_t, \mathcal{G}) \| \pi_{\theta^S}(a_t | s_t, \mathcal{G}))$$

By minimizing this loss function, the student model learns to mimic the behavior of multiple teacher models, thereby acquiring more generalized knowledge and improving its performance in multi-task learning and cross-task generalization. After each decoding step, we select the next node based on the student model’s probability distribution, transition to the new state, and repeat the aforementioned alignment process.

4 Architecture of Generalizable Multi-Task Neural Solver

Heavy decoder models have demonstrated remarkable scale generalization performance on single-task VRP. However, existing multi-task models for VRP variants predominantly rely on light encoder-heavy decoder architectures, exhibiting poor scale generalization. To address this limitation, as

depicted in Figure 2, we have developed a multi-task heavy decoder model specifically designed for VRP variants, aiming to overcome the inadequate generalization capabilities of current approaches.

4.1 Encoder

Given an instance S of the VRP, which includes N node features $(s_1 \dots s_n)$, in VRP variants, the node features are uniformly represented as (x, d, δ, s, l) , denoting the coordinate information, demand, service time, and the start and end times of the time window, respectively. These node features are then mapped through a linear layer to obtain the initial embedding $h^0 = (h_1^0 \dots h_n^0)$. Subsequently, these initial embeddings are passed through a Transformer layer to capture node relationships and generate the node embeddings. Therefore, the output of the encoder can be represented as:

$$H = \text{TF}(h^0) = (h_1, \dots, h_n)$$

where H is the matrix of final node embeddings, and h_i represents the embedding of the i -th node.

4.2 Decoder

During the decoding phase, we first extract the dynamic features $D = \{l, t, d, o\}$, encompassing the current vehicle load, current time, remaining route duration, and a binary flag indicating an open route. These dynamic features are combined with last visited node(h_{last}) and the depot node(h_{depot}) respectively, and then each combination is passed through its own linear layer. The resulting embeddings, along with the unvisited nodes($h_{unvisited}$), are processed by an L -layer Transformer network to yield updated node embeddings:

$$h^L = \text{TF}([h_{unvisited}, \text{Linear}(D \oplus h_{last}), \text{Linear}(D \oplus h_{depot})])$$

Next, we compute compatibility scores between the embeddings of all unvisited nodes and a context embedding $h_q = \text{Linear}(\text{concat}(h_{last}, h_{depot}))$ using single-head attention:

$$c(h_i^L, h_q) = \text{SHA}(h_i^L, h_q)$$

To ensure valid routes, a mask vector mask is applied to these scores. Finally, the probability $\pi(i|s_t)$ of selecting the i -th unvisited node is determined by the softmax function applied to the masked compatibility scores:

$$\pi(i|s_t) = \text{softmax}(c(h_i^L, h_q) + \text{mask}_i)$$

where $c(h_i^L, h_q)$ is the compatibility score, h_i^L is the embedding of the i -th unvisited node from h^L , and s_t is the current decoder state. The mask vector contains 0 for valid unvisited nodes and $-\infty$ for invalid ones.

To address the varying number of unvisited nodes across different instances within a batch, which can impact batch processing efficiency, we utilize padding to unify the sequence length and a masking mechanism to remove the influence of the padded depot node. Additionally, layer normalization [15] has been removed from all attention layers.

5 Random Reordering Re-Construct

Random Re-Construct (RRC) [15] is an iterative method to improve solution quality by randomly sampling and re-optimizing segments of the initial solution. RRC enhances sampling diversity via random subtour reversals and segment lengths. However, reversals can violate feasibility for some problems (e.g., VRPTW), and sampling solely on the original sequence limits diversity, hindering iterative performance. We thus propose Random Reordering Re-Construct to increase sampling diversity and improve iterative performance.

The R3C strategy is detailed in Figure 3. Given a solution, we first decompose it into subtours, then randomize their external order in the sequence. Subsequently, a random-length contiguous segment is randomly sampled and re-optimized by our model. Improved segments replace the original. By randomizing subtour order, R3C allows for more random combinations of subtours into partial solutions, aiding escape from local optima and improving iterative performance. All sampled segments end at the depot. Additionally, feasible subtour reversals are also incorporated to further enhance search diversity.

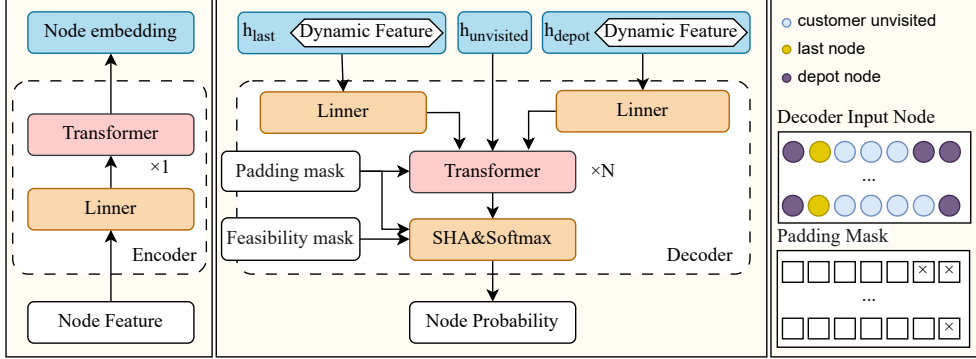


Figure 2: Architecture of the proposed multi-task neural solver. Left to right: Encoder, Decoder, Node Padding & Masking.

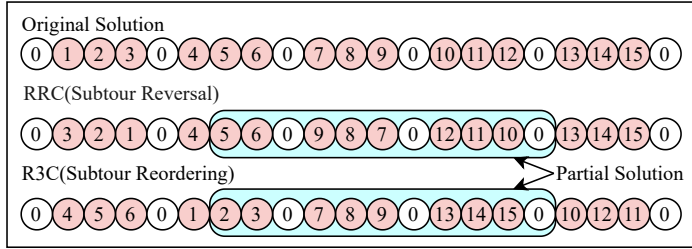


Figure 3: Comparison of RRC and R3C methods. RRC increases the diversity of sampled subproblems by randomly reversing subtours, while R3C enhances this diversity by randomly reordering the external sequence of subtours.

6 Experiments

In this section, we present a series of experiments conducted on 16 VRP variants to validate the performance of our model. All experiments are performed using one NVIDIA RTX 4090 GPU.

Baselines The baseline methods are categorized into two groups: traditional heuristic solvers and multi-task neural solvers. **(1) Traditional Solvers:** PyVRP [24]: An open-source Hybrid Genetic Search (HGS)-based solver supporting multiple complex VRP variants. It represents the current state-of-the-art in heuristic approaches for the problems considered in this study; OR-Tools [6]: Google’s open-source optimization toolkit, applicable to all VRP variants examined in this study. **(2) Multi-task Neural Solvers:** MT-POMO [11]: Multi-task extension of the POMO framework, enabling simultaneous learning across different VRP variants; MVMoE[12]: An architecture that enhances model capacity and improves performance over MT-POMO by incorporating Mixture-of-Experts (MoE) modules. Given the differences in problem variants and visible task training among the baseline models, we only compare methods with the same training setup.

Datasets We adopt the same problem settings as MVMoE[12]. We generate a test set comprising 16 VRP problems across four scales: 100, 200, 500, and 1000. The dataset at the 100-scale contains 1,000 instances, while the others contain 128 instances each. In these settings, the vehicle capacity is uniformly set to 50, the duration limit is set to 3, the time window for the depot node in Time Window problems is [0, 4.6], and for backhaul problems, the proportion of backhaul nodes is set to 20%. Our datasets are generated based on the MVMoE codebase to evaluate the performance of various baselines.

Training Configuration and Model Parameters We follow a similar setup to MVMoE, training our model on 6 VRPs and evaluating its zero-shot generalization performance on 10 unseen tasks

Table 1: Performance on seen VRPs across three scales. * represents the baseline used for gap calculation.

Method	Pro.	Problem Size			Pro.	Problem Size		
		n=100	n=500	n=1k		n=100	n=500	n=1k
HGS-PyVRP	CVRP	15.53(*)	62.07(*)	119.54(*)	VRPTW	24.35(*)	90.61(*)	166.47(*)
OR-Tools		15.94(2.63%)	66.51(7.15%)	125.91(5.32%)		25.21(3.54%)	98.45(8.65%)	178.47(7.21%)
MT-POMO(S.T.)		16.25(4.64%)	70.60(13.74%)	146.92(22.90%)		26.66(10.40%)	122.61(35.50%)	247.44(66.47%)
MT-POMO(M+aug8)		15.79(1.69%)	67.99(9.54%)	136.62(14.28%)		25.61(5.18%)	115.43(27.39%)	229.82(38.06%)
MVMoE(S.T.)		16.30(5.00%)	77.44(24.77%)	191.07(59.83%)		26.88(10.44%)	122.78(35.26%)	267.33(60.59%)
MVMoE(M+aug8)		15.76(1.50%)	73.61(18.59%)	176.40(47.57%)		25.51(4.78%)	116.67(28.76%)	253.35(52.19%)
MTL-KD ₉₆		16.06(3.41%)	64.57(4.02%)	123.88(3.63%)		26.18(7.52%)	100.17(10.55%)	188.94(13.50%)
MTL-KD ₁₂₈		16.04(3.30%)	64.61(4.09%)	124.44(4.09%)		26.13(7.32%)	99.05(9.31%)	184.92(11.09%)
MTL-KD(R3C200) ₁₂₈		15.76(1.48%)	63.63(2.51%)	122.06(2.10%)		25.31(3.93%)	96.43(6.42%)	181.85(9.24%)
HGS-PyVRP	VRPL	15.58(*)	63.55(*)	122.68(*)	VRPB	-	-	-
OR-Tools		16.00(2.69%)	67.53(6.26%)	128.16(4.46%)		11.97(*)	47.76(*)	88.57(*)
MT-POMO(S.T.)		16.29(4.52%)	71.46(12.66%)	149.55(21.90%)		12.47(4.21%)	50.08(4.85%)	99.56(12.41%)
MT-POMO(M+aug8)		15.85(1.67%)	68.95(8.49%)	138.97(13.27%)		12.04(0.63%)	48.49(1.52%)	95.35(7.64%)
MVMoE(S.T.)		16.36(4.94%)	78.79(23.97%)	192.29(56.74%)		12.42(3.80%)	71.99(50.75%)	186.49(110.54%)
MVMoE(M+aug8)		15.81(1.45%)	74.67(17.50%)	177.89(45.00%)		12.01(0.31%)	66.26(38.73%)	167.26(88.84%)
MTL-KD ₉₆		16.14(3.58%)	65.45(2.99%)	126.11(2.79%)		12.39(3.51%)	46.12(-3.44%)	86.90(-1.89%)
MTL-KD ₁₂₈		16.12(3.45%)	65.48(3.03%)	126.66(3.25%)		12.38(3.41%)	45.99(-3.70%)	86.99(-1.78%)
MTL-KD(R3C200) ₁₂₈		15.82(1.50%)	64.5246(1.53%)	124.59(1.56%)		12.02(0.43%)	44.58(-6.66%)	83.66(-5.55%)
HGS-PyVRP	OVRP	9.71(*)	35.30(*)	66.10(*)	OVRPTW	13.95(*)	48.15(*)	82.98(*)
OR-Tools		9.84(1.38%)	37.81(7.11%)	70.38(6.48%)		14.38(3.06%)	52.48(9.00%)	90.03(8.49%)
MT-POMO(S.T.)		10.66(9.83%)	44.62(26.41%)	92.78(40.36%)		15.56(11.53%)	71.63(48.76%)	147.84(78.16%)
MT-POMO(M+aug8)		10.17(4.74%)	41.93(18.78%)	85.27(29.00%)		14.85(6.43%)	66.74(38.61%)	135.99(63.87%)
MVMoE(S.T.)		10.77(10.94%)	49.35(39.81%)	135.30(104.70%)		15.70(12.54%)	82.81(71.99%)	215.21(159.34%)
MVMoE(M+aug8)		10.14(4.42%)	46.23(30.97%)	116.82(76.74%)		14.78(5.90%)	76.28(58.43%)	195.64(135.76%)
MTL-KD ₉₆		10.41(7.21%)	38.73(9.72%)	72.73(10.03%)		15.11(8.32%)	53.74(11.61%)	94.12(13.42%)
MTL-KD ₁₂₈		10.46(7.19%)	38.89(10.17%)	72.70(9.98%)		15.08(8.07%)	53.89(11.91%)	93.96(13.22%)
MTL-KD(R3C200) ₁₂₈		10.05(3.53%)	37.7934(7.07%)	71.40(8.03%)		14.53(4.12%)	52.08(8.15%)	92.40(11.35%)

(refer to Figure 1). The training process consists of two phases: teacher model pre-training and student model training. **(1) Teacher Model Pre-training:** We employ the POMO model as our teacher model. For each of the 6 visible tasks, we independently train a single-task model using reinforcement learning. All teacher models share the same parameter configuration: 6 encoder layers, 1 decoder layer, an embedding dimension of 128, 8 attention heads, and a Feedforward hidden dimension of 512. The teacher models are trained for 4000 epochs on random instances of scale 100, with 20,000 training instances per epoch, a batch size of 128, and an initial learning rate of 0.0001. **(2) Student Model Training:** The student model consists of 1 encoder layer and 6 decoder layers, with embedding dimensions set to 128 and 96, employing 8 multi-head attention heads and a Feedforward hidden dimension of 512. The student model simultaneously learns from the 6 pre-trained teacher models on datasets with a problem scale of 100. The training batch size is set to 1500 (250 * 6), with 24,000 training instances per epoch, an initial learning rate of 0.0001, and a total of 900 training epochs. After the 300th epoch, the learning rate is halved every 100 epochs.

Inference and Metrics We adopt the Average Objective Value and Gap as evaluation metrics, where smaller values indicate better performance. The Objective Value represents the total distance of the solution in the Vehicle Routing Problem, while the Gap evaluates the performance difference of each method compared to a traditional baseline method (such as HGS-PyVRP).

We test the results of a Single Trajectory Greedy Search (S.T.) on all methods. Furthermore, to compare with the results of other solvers exploring multiple trajectories under data augmentation (denoted as M × aug8, where M is the number of nodes and aug8 represents 8 types of data augmentation[8]), our method employs the R3C strategy iterated 200 times under a single trajectory

6.1 Main Results

Performance on seen Tasks We evaluate the performance of our model on the training tasks, and the results are shown in Table 1. The results demonstrate that our proposed MTL-KD model exhibits excellent performance on the seen training tasks, particularly showcasing a more pronounced advantage when dealing with larger-scale problems. This validates the effectiveness of our proposed knowledge distillation training framework and model architecture.

Performance on Unseen Tasks The zero-shot generalization experimental results on 10 unseen tasks (as shown in Table 2) indicate that our MTL-KD model outperforms the compared models in most cases, demonstrating remarkable cross-task generalization ability, especially with a significant

Table 2: Performance on unseen VRPs across three scales. * represents the baseline used for gap calculation.

Method	Pro.	Problem Size			Pro.	Problem Size		
		n=100	n=500	n=1k		n=100	n=500	n=1k
HGS-PyVRP	OVRPL	9.67(*)	34.70(*)	65.38(*)	VRPLTW	24.44(*)	91.86(*)	174.79(*)
OR-Tools		9.79(1.25%)	37.09(6.89%)	69.64(6.51%)		25.65(4.96%)	99.50(8.31%)	186.38(6.63%)
MT-POMO(S.T.)		10.61(9.69%)	43.77(26.13%)	92.49(41.45%)		26.76(9.52%)	123.97(34.95%)	252.82(44.65%)
MT-POMO(M+aug8)		10.13(4.72%)	41.28(18.95%)	84.40(29.08%)		25.71(5.21%)	116.62(26.95%)	235.94(34.99%)
MVMoE(S.T.)		10.76(11.25%)	48.60(40.05%)	135.08(106.58%)		27.00(10.48%)	124.25(35.25%)	274.68(57.15%)
MVMoE(M+aug8)		10.10(4.43%)	45.58(31.36%)	116.71(78.48%)		25.62(4.84%)	118.00(28.45%)	260.07(48.79%)
MTL-KD(S.T.) ₉₆		10.42(7.73%)	38.23(10.17%)	72.32(10.61%)		26.37(7.89%)	101.39(10.36%)	195.65(11.94%)
MTL-KD(S.T.) ₁₂₈		10.44(7.95%)	38.43(10.76%)	72.78(11.31%)		26.35(7.81%)	100.40(9.30%)	192.41(10.08%)
MTL-KD(R3C200) ₁₂₈		10.08(4.29%)	37.27(7.41%)	71.35(9.12%)		25.55(4.54%)	97.85(6.51%)	189.02(8.14%)
HGS-PyVRP	OVRPLTW	14.00(*)	47.97 (*)	83.68(*)	OVRPB	-	-	-
OR-Tools		14.28(1.98%)	52.94(10.36%)	91.69(9.57%)		8.37(*)	29.98 (*)	54.87 (*)
MT-POMO(S.T.)		15.61(11.46%)	71.24(48.52%)	147.97(76.82%)		9.52(13.82%)	35.43(18.17%)	74.59(35.95%)
MT-POMO(M+aug8)		14.90(6.39%)	66.65(38.95%)	137.13(63.87%)		8.98(7.34%)	32.76(9.28%)	66.91(21.95%)
MVMoE(S.T.)		15.74(12.39%)	82.49(71.97%)	219.21(161.95%)		9.74(16.41%)	45.80(52.76%)	129.38(135.81%)
MVMoE(M+aug8)		14.83(5.90%)	76.12(58.68%)	197.84(136.41%)		8.96(7.10%)	40.41(34.77%)	109.08(98.81%)
MTL-KD(S.T.) ₉₆		15.28(9.12%)	53.38 (11.28%)	94.65(13.11%)		9.25(10.58%)	30.90(3.08%)	58.57(6.76%)
MTL-KD(S.T.) ₁₂₈		15.26(8.95%)	53.56(11.65%)	95.33(13.92%)		9.27(10.81%)	30.45 (1.58%)	56.92 (3.73%)
MTL-KD(R3C200) ₁₂₈		14.71(5.02%)	51.97(8.34%)	93.91(12.22%)		8.78(4.95%)	28.73(-4.16%)	52.41(-4.48%)
OR-Tools	VRPBL	12.02(*)	47.93 (*)	89.82 (*)	VRPB	25.41(*)	97.77(*)	194.69(*)
MT-POMO(S.T.)		12.71(5.79%)	50.70(5.77%)	99.51(10.78%)		28.64(12.70%)	126.00(28.87%)	270.68(39.03%)
MT-POMO(M+aug8)		12.10(0.66%)	48.14(0.45%)	94.26(4.94%)		26.94(6.04%)	118.20(20.89%)	251.58(29.22%)
MVMoE(S.T.)		12.86(7.06%)	70.03(46.11%)	159.91(78.03%)		28.88(13.67%)	125.89(28.76%)	294.23(51.13%)
MVMoE(M+aug8)		12.05(0.28%)	63.57(32.63%)	145.61(62.10%)		26.89(5.82%)	119.44(22.16%)	276.17(41.85%)
MTL-KD(S.T.) ₉₆		12.56(4.54%)	45.90(4.23%)	86.45(-3.75%)		28.48(12.11%)	105.43(7.83%)	215.94(10.92%)
MTL-KD(S.T.) ₁₂₈		12.54(4.32%)	45.67(-4.72%)	86.28(-3.95%)		28.49 (12.12%)	103.85 (6.21%)	209.82(7.77%)
MTL-KD(R3C200) ₁₂₈		12.08(0.55%)	44.27(-7.64%)	82.56(-8.08%)		26.64(4.84%)	100.25(2.53%)	205.13(5.37%)
OR-Tools	OVRPBL	8.35 (*)	29.60(*)	54.30 (*)	OVRPB	14.38(*)	51.88 (*)	90.86 (*)
MT-POMO(S.T.)		9.50(13.79%)	35.34(19.37%)	74.83(37.80%)		16.92(17.64%)	72.91(40.53%)	152.63(67.98%)
MT-POMO(M+aug8)		8.96(7.35%)	32.60(10.13%)	66.87(23.13%)		15.88(10.39%)	67.95(30.96%)	140.72(54.87%)
MVMoE(S.T.)		9.75(16.75%)	45.46(53.57%)	127.34(134.49%)		17.07(18.68%)	81.57(57.22%)	214.76(136.36%)
MVMoE(M+aug8)		8.94(7.12%)	40.35(36.29%)	108.53(99.86%)		15.81(9.90%)	74.43(43.46%)	193.33(112.77%)
MTL-KD(S.T.) ₉₆		9.29(11.27%)	31.96(7.96%)	61.37(13.01%)		16.70(16.10%)	56.02(7.97%)	99.85(9.89%)
MTL-KD(S.T.) ₁₂₈		9.41(12.75%)	31.42(6.14%)	59.25(9.11%)		16.74(16.39%)	56.02(7.98%)	99.20(9.18%)
MTL-KD(R3C200) ₁₂₈		8.84(5.95%)	29.23(-1.26%)	53.77(-0.98%)		15.58(8.30%)	53.75(3.62%)	97.37(7.17%)
OR-Tools	VRPBBLT	25.34 (*)	103.17(*)	189.31(*)	OVRPB	14.25(*)	52.37(*)	92.16(*)
MT-POMO(S.T.)		28.92(14.11%)	131.68(27.64%)	264.39(39.66%)		16.78(17.79%)	73.26(39.90%)	152.61(65.60%)
MT-POMO(M+aug8)		27.25(7.52%)	123.71(19.91%)	245.61(29.74%)		15.74(10.45%)	68.08(30.01%)	141.27(53.28%)
MVMoE(S.T.)		29.19(15.18%)	132.23(28.17%)	286.27(51.21%)		16.95(18.94%)	82.36(57.28%)	215.69(134.03%)
MVMoE(M+aug8)		27.14(7.10%)	125.27(21.43%)	269.13(42.16%)		15.67(9.97%)	74.83(42.90%)	195.45(112.07%)
MTL-KD(S.T.) ₉₆		29.01(14.4703%)	111.33(7.92%)	210.45(11.17%)		16.78(17.74%)	56.34(7.59%)	101.43 (10.06%)
MTL-KD(S.T.) ₁₂₈		29.13 (14.96%)	110.33 (6.94%)	205.52 (8.56%)		16.95(18.93%)	57.15(9.13%)	101.64(10.29%)
MTL-KD(R3C200) ₁₂₈		27.12(7.03%)	106.52(3.26%)	201.29(6.33%)		15.65 (9.84%)	54.68(4.41%)	99.64(8.11%)

advantage on large-scale problems. This validates that multi-task knowledge distillation training endows the model with strong generalization capabilities across different VRP variants.

Performance on Real-World Instances We also evaluate the performance of our model on real-world datasets, including Set-X (medium and large scale) from CVRPLIB[25] for CVRP and the Solomon dataset[26] for VRPTW. We compare our model against several single-task and multi-task models, and the experimental results are presented in Tables 5, 6, and 7, AppendixC. Our model consistently outperforms other single-task and multi-task models across all three real-world datasets, demonstrating particularly strong performance on the large-scale Set-X dataset, where the gap is significantly smaller than other baselines. This indicates the strong applicability of our approach to real-world scenarios.

6.2 Ablation Study

Scale Generalization Comparison: Student vs. Teacher While heavy decoders are generally considered to have significant potential for large-scale generalization, our model’s learning teacher model, POMO, primarily excels at its specific training scale and lacks cross-scale generalization capabilities. This naturally raises a crucial question: will the student model also be limited to learning knowledge specific to a particular scale, thereby restricting its generalization ability? To investigate this, we compare the performance of several single-task teacher models with our MTL-KD model on the same dataset, as shown in Figure 4. In contrast to the teacher models, the student model demonstrates a notable capacity for scale generalization. This observation indicates that the MTL-KD model, during the learning process, does not simply replicate the teacher’s knowledge but rather effectively adapts to variations in scale, consequently achieving robust generalization performance.

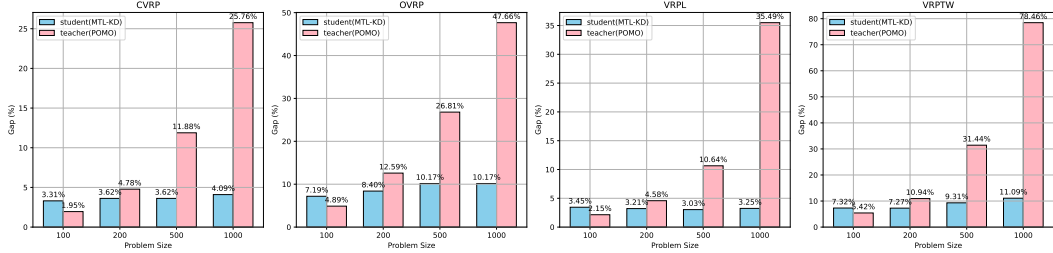


Figure 4: Performance Comparison between Teacher and Student Models, both trained on instances of scale 100.

Performance Comparison: KD vs. RL To highlight the effectiveness of our knowledge distillation approach, we compared the MTL-KD model with a LEHD model trained using RL. Given the high computational cost associated with training the LEHD model with RL, we were only able to train it at a scale of 20. Subsequently, we evaluated the average gap of both models on all seen and unseen tasks, with the experimental results presented in Table 3. The results indicate that the RL method, due to its limitation to training on small scales, struggles to leverage the full potential of the LEHD model, leading to significantly poor performance. In contrast, our distillation-based MTL-KD model demonstrates a clear performance advantage.

Table 3: Heavy Decoder Performance (RL vs. KD) on Seen/Unseen Tasks (Average Gap).

Problem Size		100	200	500	1000
Training task	RLMT-LEHD	21.7834%	27.2457%	38.2808%	50.0606%
	MTL-KD	5.4569%	5.2775%	5.8028%	6.6413%
unseen task	RLMT-LEHD	31.2513%	37.1404%	48.9074%	62.2226%
	MTL-KD	19.1658%	12.9145%	10.8275%	13.3322%

Effectiveness Analysis of R3C To validate the effectiveness of our proposed R3C method, we conduct experiments on CVRP, VRPL, OVRP, and VRPTW at a scale of 100. We perform an ablation study on the random reordering of the subtour external order component, with the following comparative experiments: random sampling on the original solution only (RS); random reordering of the subtour external order followed by sampling (RS+Ro); and for CVRP and VRPL, we also analyze the impact of adding a random flipping operation (F) since it does not affect the legality of the solution. The experimental results are shown in Figure 5. Incorporating the random reordering operation significantly improves the iterative performance during reconstruction, which benefits from the ability of random reordering to enhance the diversity of sampled subproblems. Furthermore, the random flipping operation can moderately increase the diversity of sampled solutions when only initial solution random sampling is performed; however, its impact is minimal with random reordering, further confirming the effectiveness of the random reordering operation.

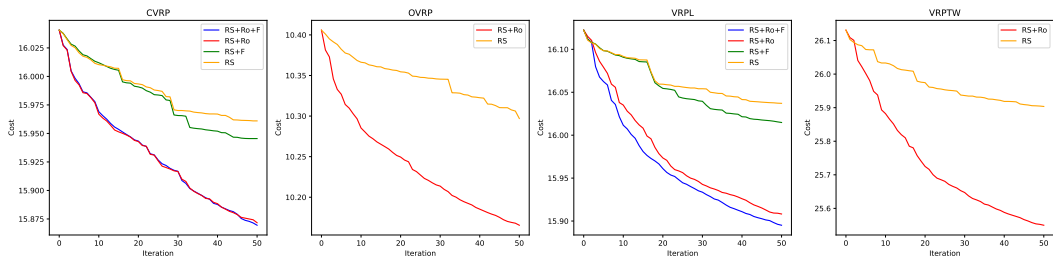


Figure 5: Impact of Different Components in R3C.

7 Conclusion

This paper implements a heavy decoder model in the multi-task VRP domain and achieves label-free training of this heavy decoder model through a multi-task knowledge distillation method. The proposed approach demonstrates excellent performance on seen tasks, unseen tasks, and real-world datasets, exhibiting significant large-scale generalization ability, thereby validating the effectiveness of our method. Furthermore, the proposed R3C method further enhances the model’s performance. However, the structure of the heavy decoder leads to high computational complexity, which is a limitation. Future work will explore how to implement more efficient and robust model architectures in the multi-task domain.

References

- [1] Diego Cattaruzza, Nabil Absi, Dominique Feillet, and Jesús González-Feliu. Vehicle routing problems for city logistics. *EURO Journal on Transportation and Logistics*, 6(1):51–79, 2017.
- [2] Mouhcine Elgarej, Mansouri Khalifa, and Mohamed Youssfi. Optimized path planning for electric vehicle routing and charging station navigation systems. In *Research Anthology on Architectures, Frameworks, and Integration Strategies for Distributed and Cloud Computing*, pages 1945–1967. IGI Global, 2021.
- [3] Jianan Zhou, Yaxin Wu, Zhiguang Cao, Wen Song, Jie Zhang, and Zhenghua Chen. Learning large neighborhood search for vehicle routing in airport ground handling. *IEEE Transactions on knowledge and data engineering*, 35(9):9769–9782, 2023.
- [4] Keld Helsgaun. An extension of the lin-kernighan-helsgaun tsp solver for constrained traveling salesman and vehicle routing problems. *Roskilde: Roskilde University*, 12:966–980, 2017.
- [5] Thibaut Vidal. Hybrid genetic search for the cvrp: Open-source implementation and swap* neighborhood. *Computers & Operations Research*, 140:105643, 2022.
- [6] Vincent Furnon and Laurent Perron. Or-tools routing library, 2023. URL <https://developers.google.com/optimization/routing>.
- [7] Wouter Kool, Herke van Hoof, and Max Welling. Attention, learn to solve routing problems! In *International Conference on Learning Representations*, 2019.
- [8] Yeong-Dae Kwon, Jinho Choo, Byoungjip Kim, Iljoo Yoon, Youngjune Gwon, and Seungjai Min. Pomo: Policy optimization with multiple optima for reinforcement learning. *Advances in Neural Information Processing Systems*, 33:21188–21198, 2020.
- [9] Minsu Kim, Junyoung Park, and Jinkyoo Park. Sym-nco: Leveraging symmetry for neural combinatorial optimization. *Advances in Neural Information Processing Systems*, 35:1936–1949, 2022.
- [10] Yan Jin, Yuandong Ding, Xuanhao Pan, Kun He, Li Zhao, Tao Qin, Lei Song, and Jiang Bian. Pointerformer: Deep reinforced multi-pointer transformer for the traveling salesman problem. *Proceedings of the AAAI Conference on Artificial Intelligence*, 37(7):8132–8140, 2023.
- [11] Fei Liu, Xi Lin, Qingfu Zhang, Xialiang Tong, and Mingxuan Yuan. Multi-task learning for routing problem with cross-problem zero-shot generalization. *International Conference on Knowledge Discovery and Data Mining (KDD)*, 2024.
- [12] Jianan Zhou, Zhiguang Cao, Yaxin Wu, Wen Song, Yining Ma, Jie Zhang, and Chi Xu. Mvmoe: multi-task vehicle routing solver with mixture-of-experts. In *Proceedings of the 41st International Conference on Machine Learning*, pages 61804–61824, 2024.
- [13] Federico Berto, Chuanbo Hua, Nayeli Gast Zepeda, André Hottung, Niels Wouda, Leon Lan, Junyoung Park, Kevin Tierney, and Jinkyoo Park. Routefinder: Towards foundation models for vehicle routing problems. *arXiv preprint arXiv:2406.15007*, 2024.
- [14] Ziwei Huang, Jianan Zhou, Zhiguang Cao, and Yixin XU. Rethinking light decoder-based solvers for vehicle routing problems. In *The Thirteenth International Conference on Learning Representations*, 2025.
- [15] Fu Luo, Xi Lin, Fei Liu, Qingfu Zhang, and Zhenkun Wang. Neural combinatorial optimization with heavy decoder: Toward large scale generalization. In A. Oh, T. Naumann, A. Globerson, K. Saenko, M. Hardt, and S. Levine, editors, *Advances in Neural Information Processing Systems*, volume 36, pages 8845–8864. Curran Associates, Inc., 2023.

[16] Darko Drakulic, Sofia Michel, Florian Mai, Arnaud Sors, and Jean-Marc Andreoli. Bq-nco: Bisimulation quotienting for efficient neural combinatorial optimization. In A. Oh, T. Naumann, A. Globerson, K. Saenko, M. Hardt, and S. Levine, editors, *Advances in Neural Information Processing Systems*, volume 36, pages 77416–77429. Curran Associates, Inc., 2023.

[17] Fu Luo, Xi Lin, Yaxin Wu, Zhenkun Wang, Tong Xialiang, Mingxuan Yuan, and Qingfu Zhang. Boosting neural combinatorial optimization for large-scale vehicle routing problems. In *The Thirteenth International Conference on Learning Representations*, 2025.

[18] Geoffrey E. Hinton, Oriol Vinyals, and J. Michael Dean. Distilling the knowledge in a neural network. *arXiv: Machine Learning, arXiv: Machine Learning*, Mar 2015.

[19] Jieyi Bi, Yining Ma, Jiahai Wang, Zhiguang Cao, Jinbiao Chen, Yuan Sun, and Yeow Meng Chee. Learning generalizable models for vehicle routing problems via knowledge distillation. *Advances in Neural Information Processing Systems*, 35:31226–31238, 2022.

[20] Yubin Xiao, Di Wang, Boyang Li, Mingzhao Wang, Xuan Wu, Changliang Zhou, and You Zhou. Distilling autoregressive models to obtain high-performance non-autoregressive solvers for vehicle routing problems with faster inference speed. *Proceedings of the AAAI Conference on Artificial Intelligence*, 38(18):20274–20283, 2024.

[21] Qidong Liu, Xin Shen, Chaoyue Liu, Dong Chen, Xin Zhou, and Mingliang Xu. Enhancing the generalization capability of 2d array pointer networks through multiple teacher-forcing knowledge distillation. *Journal of Automation and Intelligence*, 2025.

[22] Sisi Zheng and Rongye Ye. Aspdd: An adaptive knowledge distillation framework for tsp generalization problems. *IEEE Access*, 2024.

[23] Ronald J Williams. Simple statistical gradient-following algorithms for connectionist reinforcement learning. *Machine learning*, 8:229–256, 1992.

[24] Niels A Wouda, Leon Lan, and Wouter Kool. PyVRP: A high-performance VRP solver package. *INFORMS Journal on Computing*, 2024.

[25] Eduardo Uchoa, Diego Pecin, Artur Pessoa, Marcus Poggi, Thibaut Vidal, and Anand Subramanian. New benchmark instances for the capacitated vehicle routing problem. *European Journal of Operational Research*, 257(3):845–858, 2017.

[26] Marius M Solomon. Algorithms for the vehicle routing and scheduling problems with time window constraints. *Operations research*, 35(2):254–265, 1987.

[27] Oriol Vinyals, Meire Fortunato, and Navdeep Jaitly. Pointer networks. *Advances in neural information processing systems*, 28, 2015.

[28] Irwan Bello, Hieu Pham, Quoc V. Le, Mohammad Norouzi, and Samy Bengio. Neural combinatorial optimization with reinforcement learning. In *International Conference on Learning Representations Workshop Track*, 2017. URL https://openreview.net/forum?id=HyG_D4v9xx.

[29] Mohammadreza Nazari, Afshin Oroojlooy, Lawrence Snyder, and Martin Takáć. Reinforcement learning for solving the vehicle routing problem. *Advances in neural information processing systems*, 31, 2018.

[30] Yeong-Dae Kwon, Jinho Choo, Iljoo Yoon, Minah Park, Duwon Park, and Youngjune Gwon. Matrix encoding networks for neural combinatorial optimization. *Advances in Neural Information Processing Systems*, 34:5138–5149, 2021.

[31] Liang Xin, Wen Song, Zhiguang Cao, and Jie Zhang. Multi-decoder attention model with embedding glimpse for solving vehicle routing problems. *Proceedings of the AAAI Conference on Artificial Intelligence*, 35(13):12042–12049, 2021.

[32] Jianan Zhou, Yaxin Wu, Wen Song, Zhiguang Cao, and Jie Zhang. Towards omni-generalizable neural methods for vehicle routing problems. In *International Conference on Machine Learning*, pages 42769–42789. PMLR, 2023.

[33] Rui Sun, Zhi Zheng, and Zhenkun Wang. Learning encodings for constructive neural combinatorial optimization needs to regret. *Proceedings of the AAAI Conference on Artificial Intelligence*, 38(18):20803–20811, 2024.

[34] Zhi Zheng, Shunyu Yao, Zhenkun Wang, Tong Xialiang, Mingxuan Yuan, and Ke Tang. DPN: Decoupling partition and navigation for neural solvers of min-max vehicle routing problems. In *Forty-first International Conference on Machine Learning*, 2024. URL <https://openreview.net/forum?id=ar174skI9u>.

[35] Chengrui Gao, Haopu Shang, Ke Xue, Dong Li, and Chao Qian. Towards generalizable neural solvers for vehicle routing problems via ensemble with transferrable local policy. In *Proceedings of the Thirty-Third International Joint Conference on Artificial Intelligence*, pages 6914–6922, 2024.

[36] Han Fang, Zhihao Song, Paul Weng, and Yutong Ban. Invit: a generalizable routing problem solver with invariant nested view transformer. In *Proceedings of the 41st International Conference on Machine Learning*, pages 12973–12992, 2024.

[37] Changliang Zhou, Xi Lin, Zhenkun Wang, Xialiang Tong, Mingxuan Yuan, and Qingfu Zhang. Instance-conditioned adaptation for large-scale generalization of neural combinatorial optimization. *arXiv preprint arXiv:2405.01906*, 2024.

[38] Qingchun Hou, Jingwei Yang, Yiqiang Su, Xiaoqing Wang, and Yuming Deng. Generalize learned heuristics to solve large-scale vehicle routing problems in real-time. In *The Eleventh International Conference on Learning Representations*, 2023.

[39] Haoran Ye, Jiarui Wang, Helan Liang, Zhiguang Cao, Yong Li, and Fanzhang Li. Glop: Learning global partition and local construction for solving large-scale routing problems in real-time. *Proceedings of the AAAI Conference on Artificial Intelligence*, 38(18):20284–20292, 2024.

[40] Zhi Zheng, Changliang Zhou, Xialiang Tong, Mingxuan Yuan, and Zhenkun Wang. Udc: A unified neural divide-and-conquer framework for large-scale combinatorial optimization problems. In A. Globerson, L. Mackey, D. Belgrave, A. Fan, U. Paquet, J. Tomczak, and C. Zhang, editors, *Advances in Neural Information Processing Systems*, volume 37, pages 6081–6125. Curran Associates, Inc., 2024.

[41] Chenguang Wang and Tianshu Yu. Efficient training of multi-task combinatorial neural solver with multi-armed bandits. *arXiv preprint arXiv:2305.06361*, 2023.

[42] Zhuoyi Lin, Yaxin Wu, Bangjian Zhou, Zhiguang Cao, Wen Song, Yingqian Zhang, and Jayavelu Senthilnath. Cross-problem learning for solving vehicle routing problems. In *The 33rd International Joint Conference on Artificial Intelligence (IJCAI-24)*, 2024.

[43] Han Li, Fei Liu, Zhi Zheng, Yu Zhang, and Zhenkun Wang. Cada: Cross-problem routing solver with constraint-aware dual-attention. *arXiv preprint arXiv:2412.00346*, 2024.

NeurIPS Paper Checklist

1. Claims

Question: Do the main claims made in the abstract and introduction accurately reflect the paper's contributions and scope?

Answer: **[Yes]**

Justification: The main claims made in the abstract and introduction accurately reflect the contributions and scope of the paper.

Guidelines:

- The answer NA means that the abstract and introduction do not include the claims made in the paper.
- The abstract and/or introduction should clearly state the claims made, including the contributions made in the paper and important assumptions and limitations. A No or NA answer to this question will not be perceived well by the reviewers.
- The claims made should match theoretical and experimental results, and reflect how much the results can be expected to generalize to other settings.
- It is fine to include aspirational goals as motivation as long as it is clear that these goals are not attained by the paper.

2. Limitations

Question: Does the paper discuss the limitations of the work performed by the authors?

Answer: **[Yes]**

Justification: The paper discusses the limitations of the work in the last section.

Guidelines:

- The answer NA means that the paper has no limitation while the answer No means that the paper has limitations, but those are not discussed in the paper.
- The authors are encouraged to create a separate "Limitations" section in their paper.
- The paper should point out any strong assumptions and how robust the results are to violations of these assumptions (e.g., independence assumptions, noiseless settings, model well-specification, asymptotic approximations only holding locally). The authors should reflect on how these assumptions might be violated in practice and what the implications would be.
- The authors should reflect on the scope of the claims made, e.g., if the approach was only tested on a few datasets or with a few runs. In general, empirical results often depend on implicit assumptions, which should be articulated.
- The authors should reflect on the factors that influence the performance of the approach. For example, a facial recognition algorithm may perform poorly when image resolution is low or images are taken in low lighting. Or a speech-to-text system might not be used reliably to provide closed captions for online lectures because it fails to handle technical jargon.
- The authors should discuss the computational efficiency of the proposed algorithms and how they scale with dataset size.
- If applicable, the authors should discuss possible limitations of their approach to address problems of privacy and fairness.
- While the authors might fear that complete honesty about limitations might be used by reviewers as grounds for rejection, a worse outcome might be that reviewers discover limitations that aren't acknowledged in the paper. The authors should use their best judgment and recognize that individual actions in favor of transparency play an important role in developing norms that preserve the integrity of the community. Reviewers will be specifically instructed to not penalize honesty concerning limitations.

3. Theory assumptions and proofs

Question: For each theoretical result, does the paper provide the full set of assumptions and a complete (and correct) proof?

Answer: **[NA]**

Justification: The paper does not include theoretical results

Guidelines:

- The answer NA means that the paper does not include theoretical results.
- All the theorems, formulas, and proofs in the paper should be numbered and cross-referenced.
- All assumptions should be clearly stated or referenced in the statement of any theorems.
- The proofs can either appear in the main paper or the supplemental material, but if they appear in the supplemental material, the authors are encouraged to provide a short proof sketch to provide intuition.
- Inversely, any informal proof provided in the core of the paper should be complemented by formal proofs provided in appendix or supplemental material.
- Theorems and Lemmas that the proof relies upon should be properly referenced.

4. Experimental result reproducibility

Question: Does the paper fully disclose all the information needed to reproduce the main experimental results of the paper to the extent that it affects the main claims and/or conclusions of the paper (regardless of whether the code and data are provided or not)?

Answer: [Yes]

Justification: We will make our code, datasets, and pre-trained models publicly available upon final manuscript submission, with all implementation details thoroughly described in the paper.

Guidelines:

- The answer NA means that the paper does not include experiments.
- If the paper includes experiments, a No answer to this question will not be perceived well by the reviewers: Making the paper reproducible is important, regardless of whether the code and data are provided or not.
- If the contribution is a dataset and/or model, the authors should describe the steps taken to make their results reproducible or verifiable.
- Depending on the contribution, reproducibility can be accomplished in various ways. For example, if the contribution is a novel architecture, describing the architecture fully might suffice, or if the contribution is a specific model and empirical evaluation, it may be necessary to either make it possible for others to replicate the model with the same dataset, or provide access to the model. In general, releasing code and data is often one good way to accomplish this, but reproducibility can also be provided via detailed instructions for how to replicate the results, access to a hosted model (e.g., in the case of a large language model), releasing of a model checkpoint, or other means that are appropriate to the research performed.
- While NeurIPS does not require releasing code, the conference does require all submissions to provide some reasonable avenue for reproducibility, which may depend on the nature of the contribution. For example
 - (a) If the contribution is primarily a new algorithm, the paper should make it clear how to reproduce that algorithm.
 - (b) If the contribution is primarily a new model architecture, the paper should describe the architecture clearly and fully.
 - (c) If the contribution is a new model (e.g., a large language model), then there should either be a way to access this model for reproducing the results or a way to reproduce the model (e.g., with an open-source dataset or instructions for how to construct the dataset).
 - (d) We recognize that reproducibility may be tricky in some cases, in which case authors are welcome to describe the particular way they provide for reproducibility. In the case of closed-source models, it may be that access to the model is limited in some way (e.g., to registered users), but it should be possible for other researchers to have some path to reproducing or verifying the results.

5. Open access to data and code

Question: Does the paper provide open access to the data and code, with sufficient instructions to faithfully reproduce the main experimental results, as described in supplemental material?

Answer: [No]

Justification: We will release the dataset and code upon manuscript acceptance, with all experimental details documented in the paper to ensure full reproducibility of our results.

Guidelines:

- The answer NA means that paper does not include experiments requiring code.
- Please see the NeurIPS code and data submission guidelines (<https://nips.cc/public/guides/CodeSubmissionPolicy>) for more details.
- While we encourage the release of code and data, we understand that this might not be possible, so “No” is an acceptable answer. Papers cannot be rejected simply for not including code, unless this is central to the contribution (e.g., for a new open-source benchmark).
- The instructions should contain the exact command and environment needed to run to reproduce the results. See the NeurIPS code and data submission guidelines (<https://nips.cc/public/guides/CodeSubmissionPolicy>) for more details.
- The authors should provide instructions on data access and preparation, including how to access the raw data, preprocessed data, intermediate data, and generated data, etc.
- The authors should provide scripts to reproduce all experimental results for the new proposed method and baselines. If only a subset of experiments are reproducible, they should state which ones are omitted from the script and why.
- At submission time, to preserve anonymity, the authors should release anonymized versions (if applicable).
- Providing as much information as possible in supplemental material (appended to the paper) is recommended, but including URLs to data and code is permitted.

6. Experimental setting/details

Question: Does the paper specify all the training and test details (e.g., data splits, hyper-parameters, how they were chosen, type of optimizer, etc.) necessary to understand the results?

Answer: [Yes]

Justification: Both the testing and training settings are detailed in Section Experiment 6

Guidelines:

- The answer NA means that the paper does not include experiments.
- The experimental setting should be presented in the core of the paper to a level of detail that is necessary to appreciate the results and make sense of them.
- The full details can be provided either with the code, in appendix, or as supplemental material.

7. Experiment statistical significance

Question: Does the paper report error bars suitably and correctly defined or other appropriate information about the statistical significance of the experiments?

Answer: [No]

Justification: Neural Combinatorial Optimization (NCO) methods typically only report the mean or the gap to the optimal solution (or the best-known solution). In this method, there is no randomness involved, and all random seeds are fixed at 2025.

Guidelines:

- The answer NA means that the paper does not include experiments.
- The authors should answer “Yes” if the results are accompanied by error bars, confidence intervals, or statistical significance tests, at least for the experiments that support the main claims of the paper.

- The factors of variability that the error bars are capturing should be clearly stated (for example, train/test split, initialization, random drawing of some parameter, or overall run with given experimental conditions).
- The method for calculating the error bars should be explained (closed form formula, call to a library function, bootstrap, etc.)
- The assumptions made should be given (e.g., Normally distributed errors).
- It should be clear whether the error bar is the standard deviation or the standard error of the mean.
- It is OK to report 1-sigma error bars, but one should state it. The authors should preferably report a 2-sigma error bar than state that they have a 96% CI, if the hypothesis of Normality of errors is not verified.
- For asymmetric distributions, the authors should be careful not to show in tables or figures symmetric error bars that would yield results that are out of range (e.g. negative error rates).
- If error bars are reported in tables or plots, The authors should explain in the text how they were calculated and reference the corresponding figures or tables in the text.

8. Experiments compute resources

Question: For each experiment, does the paper provide sufficient information on the computer resources (type of compute workers, memory, time of execution) needed to reproduce the experiments?

Answer: [\[Yes\]](#)

Justification: We describe the required computational resources for the experiments in the experimental section 6.

Guidelines:

- The answer NA means that the paper does not include experiments.
- The paper should indicate the type of compute workers CPU or GPU, internal cluster, or cloud provider, including relevant memory and storage.
- The paper should provide the amount of compute required for each of the individual experimental runs as well as estimate the total compute.
- The paper should disclose whether the full research project required more compute than the experiments reported in the paper (e.g., preliminary or failed experiments that didn't make it into the paper).

9. Code of ethics

Question: Does the research conducted in the paper conform, in every respect, with the NeurIPS Code of Ethics <https://neurips.cc/public/EthicsGuidelines>?

Answer: [\[Yes\]](#)

Justification: This paper strictly adheres to the standards of academic writing, especially the NeurIPS Code of Ethics.

Guidelines:

- The answer NA means that the authors have not reviewed the NeurIPS Code of Ethics.
- If the authors answer No, they should explain the special circumstances that require a deviation from the Code of Ethics.
- The authors should make sure to preserve anonymity (e.g., if there is a special consideration due to laws or regulations in their jurisdiction).

10. Broader impacts

Question: Does the paper discuss both potential positive societal impacts and negative societal impacts of the work performed?

Answer: [\[Yes\]](#)

Justification: This work focuses on solving and optimizing combinatorial optimization (CO) problems, which holds the potential to significantly enhance real-world applications. It appears to have no negative social impact. More discussion refers to Appendix E.

Guidelines:

- The answer NA means that there is no societal impact of the work performed.
- If the authors answer NA or No, they should explain why their work has no societal impact or why the paper does not address societal impact.
- Examples of negative societal impacts include potential malicious or unintended uses (e.g., disinformation, generating fake profiles, surveillance), fairness considerations (e.g., deployment of technologies that could make decisions that unfairly impact specific groups), privacy considerations, and security considerations.
- The conference expects that many papers will be foundational research and not tied to particular applications, let alone deployments. However, if there is a direct path to any negative applications, the authors should point it out. For example, it is legitimate to point out that an improvement in the quality of generative models could be used to generate deepfakes for disinformation. On the other hand, it is not needed to point out that a generic algorithm for optimizing neural networks could enable people to train models that generate Deepfakes faster.
- The authors should consider possible harms that could arise when the technology is being used as intended and functioning correctly, harms that could arise when the technology is being used as intended but gives incorrect results, and harms following from (intentional or unintentional) misuse of the technology.
- If there are negative societal impacts, the authors could also discuss possible mitigation strategies (e.g., gated release of models, providing defenses in addition to attacks, mechanisms for monitoring misuse, mechanisms to monitor how a system learns from feedback over time, improving the efficiency and accessibility of ML).

11. Safeguards

Question: Does the paper describe safeguards that have been put in place for responsible release of data or models that have a high risk for misuse (e.g., pretrained language models, image generators, or scraped datasets)?

Answer: [NA]

Justification: The paper does not pose such risks.

Guidelines:

- The answer NA means that the paper poses no such risks.
- Released models that have a high risk for misuse or dual-use should be released with necessary safeguards to allow for controlled use of the model, for example by requiring that users adhere to usage guidelines or restrictions to access the model or implementing safety filters.
- Datasets that have been scraped from the Internet could pose safety risks. The authors should describe how they avoided releasing unsafe images.
- We recognize that providing effective safeguards is challenging, and many papers do not require this, but we encourage authors to take this into account and make a best faith effort.

12. Licenses for existing assets

Question: Are the creators or original owners of assets (e.g., code, data, models), used in the paper, properly credited and are the license and terms of use explicitly mentioned and properly respected?

Answer: [Yes]

Justification: We list the licenses in Appendix D.

Guidelines:

- The answer NA means that the paper does not use existing assets.
- The authors should cite the original paper that produced the code package or dataset.
- The authors should state which version of the asset is used and, if possible, include a URL.
- The name of the license (e.g., CC-BY 4.0) should be included for each asset.

- For scraped data from a particular source (e.g., website), the copyright and terms of service of that source should be provided.
- If assets are released, the license, copyright information, and terms of use in the package should be provided. For popular datasets, paperswithcode.com/datasets has curated licenses for some datasets. Their licensing guide can help determine the license of a dataset.
- For existing datasets that are re-packaged, both the original license and the license of the derived asset (if it has changed) should be provided.
- If this information is not available online, the authors are encouraged to reach out to the asset's creators.

13. New assets

Question: Are new assets introduced in the paper well documented and is the documentation provided alongside the assets?

Answer: [NA]

Justification: The paper does not introduce new assets.

Guidelines:

- The answer NA means that the paper does not release new assets.
- Researchers should communicate the details of the dataset/code/model as part of their submissions via structured templates. This includes details about training, license, limitations, etc.
- The paper should discuss whether and how consent was obtained from people whose asset is used.
- At submission time, remember to anonymize your assets (if applicable). You can either create an anonymized URL or include an anonymized zip file.

14. Crowdsourcing and research with human subjects

Question: For crowdsourcing experiments and research with human subjects, does the paper include the full text of instructions given to participants and screenshots, if applicable, as well as details about compensation (if any)?

Answer: [NA]

Justification: The paper does not involve crowdsourcing or research involving human subjects.

Guidelines:

- The answer NA means that the paper does not involve crowdsourcing nor research with human subjects.
- Including this information in the supplemental material is fine, but if the main contribution of the paper involves human subjects, then as much detail as possible should be included in the main paper.
- According to the NeurIPS Code of Ethics, workers involved in data collection, curation, or other labor should be paid at least the minimum wage in the country of the data collector.

15. Institutional review board (IRB) approvals or equivalent for research with human subjects

Question: Does the paper describe potential risks incurred by study participants, whether such risks were disclosed to the subjects, and whether Institutional Review Board (IRB) approvals (or an equivalent approval/review based on the requirements of your country or institution) were obtained?

Answer: [NA]

Justification: The paper does not involve crowdsourcing or research involving human subjects.

Guidelines:

- The answer NA means that the paper does not involve crowdsourcing nor research with human subjects.

- Depending on the country in which research is conducted, IRB approval (or equivalent) may be required for any human subjects research. If you obtained IRB approval, you should clearly state this in the paper.
- We recognize that the procedures for this may vary significantly between institutions and locations, and we expect authors to adhere to the NeurIPS Code of Ethics and the guidelines for their institution.
- For initial submissions, do not include any information that would break anonymity (if applicable), such as the institution conducting the review.

16. Declaration of LLM usage

Question: Does the paper describe the usage of LLMs if it is an important, original, or non-standard component of the core methods in this research? Note that if the LLM is used only for writing, editing, or formatting purposes and does not impact the core methodology, scientific rigorousness, or originality of the research, declaration is not required.

Answer: [NA]

Justification: The paper does not describe the usage of LLMs as an important, original, or non-standard component of the core methods in this research.

Guidelines:

- The answer NA means that the core method development in this research does not involve LLMs as any important, original, or non-standard components.
- Please refer to our LLM policy (<https://neurips.cc/Conferences/2025/LLM>) for what should or should not be described.

A Related work

A.1 Autoregressive Neural Solvers

Autoregressive neural solvers have emerged as a prominent research direction in the field of NCO. These methods typically employ an encoder-decoder architecture, where the encoder generates node embeddings, and the decoder dynamically produces a sequence of nodes.

Early works were based on Pointer Networks[27], gradually evolving from supervised learning to reinforcement learning training[28, 29]. Subsequently, the Transformer framework was introduced and has become a mainstream paradigm[7]. POMO[8] further leverages the symmetry of the VRP, optimizing the baseline calculation in RL training and enhancing the exploration diversity of the model. Subsequent research has largely focused on improving the Transformer framework [30, 31, 10, 9, 32–34]. However, these approaches predominantly adopt a heavy encoder light decoder structure, which poses challenges in handling large-scale problems. To enhance the capability of addressing large instances, some methods continue to build upon HELD. Examples include ELG[35], which integrates local search strategies; INVIT[36], which utilizes K-nearest neighbor multi-view embeddings to enhance local information; and ICAM[37], which introduces instance-conditional adaptation to better perceive problem scales. On the other hand, some studies[15, 16] have explored heavy decoder architectures. By dynamically capturing the relationships between remaining nodes during the decoding process, these methods demonstrate superior generalization performance on large-scale problems. However, their high computational demands, often necessitating training on labeled data, represent a significant limitation. Furthermore, decomposition-based methods[38–40, 17] warrant attention. These approaches decompose large-scale problems into multiple smaller subproblems for solving, and autoregressive solvers can be employed at the lower level to address these subproblems.

A.2 Multi-Task Learning for Solving VRPs

To enhance the generalizability of neural solvers across diverse VRP variants, several existing methods have proposed unified multi-task models. For instance, Wang et al.[41] employs a multi-armed bandit approach to achieve efficient training across multiple combinatorial optimization problems. Lin et al.[42] pre-train a Transformer backbone on the Traveling Salesman Problem and fine-tune it for specific VRP variants, thereby extending its applicability to a subset of VRP problems. These methods represent initial attempts at cross-problem learning but are limited in scope, focusing primarily on a small number of problems. Building on these foundations, MT-POMO [11] views VRP variants as combinations of distinct attributes, enabling unified representation and zero-shot generalization across multiple VRP problems, achieving notable performance on ten tasks. MVMoE [12] further boosts model capacity and multi-task performance by introducing a mixture-of-experts model. RouteFinder[13] enhances multi-task training efficiency and performance through mixed batch training and enables rapid adaptation to unseen tasks via efficient adapter layers. CaDA [43] improves the model’s ability to handle diverse tasks within a multi-task framework by incorporating constraint awareness and a dual-branch structure. However, these studies have predominantly focused on small-scale problems, lacking extensive exploration of large-scale generalization capabilities.

B Problem Definition and Settings

Our VRP variant problem settings follow the work of Zhou et al. [12]. Detailed settings are as follows:

- **Coordinates:** All node coordinates are uniformly sampled from the 2D space $[0, 1] \times [0, 1]$.
- **Demands:** For all customer nodes, demands are randomly sampled from the set $\{1, 2, \dots, 9\}$.
- **Vehicle Capacity:** Each vehicle has a fixed transportation capacity, which we set to 50 across all problem scales. The sum of demands for nodes visited by a vehicle must be less than or equal to its current capacity.
- **Open Routes:** In open vehicle routing problems, vehicles are not required to return to the depot. We use a binary flag vector to distinguish whether a path is open; setting it to 1 indicates an open path.

Table 4: 16 VRP variants with five constraints.

Constraint	Capacity	Open Route	Backhaul	Duration Limit	Time Window
CVRP	✓				
OVRP	✓	✓			
VRPB	✓		✓		
VRPL	✓			✓	
VRPTW	✓				
OVRPTW	✓	✓			✓
OVRPB	✓	✓	✓		
OVRPL	✓	✓		✓	
VRPBL	✓		✓	✓	
VRPBTLW	✓		✓		
VRPLTW	✓			✓	✓
OVRPBL	✓	✓	✓	✓	
OVRPBTLW	✓	✓	✓		✓
OVRPLTW	✓	✓		✓	✓
VRPBTLW	✓		✓	✓	✓
OVRPBTLW	✓	✓	✓	✓	✓

- **Backhauls:** In problems involving backhauls, a portion of the nodes have negative demands, referred to as backhaul nodes. We designate 20% of the customer nodes as backhaul nodes, whose demands are randomly sampled from $\{-1, -2, \dots, -9\}$.
- **Duration Limit:** Each vehicle has a maximum travel distance limit, which we set to 3.
- **Time Windows:** Customer node time windows are uniformly sampled, and service time is uniformly set to 0.2. Vehicles must visit nodes within their time windows; if a vehicle arrives early, it must wait until the earliest start time. The depot’s time window is set to $[0, 3]$, with a service time of 0. Vehicle speed is uniformly set to 1, meaning the time spent traveling on a path equals its distance divided by speed. Notably, for non-open problems, it is crucial to ensure that after visiting the last customer node, the vehicle can return to the depot within its latest allowable time window; this consideration is not necessary for open problems.

By combining different constraints, 16 VRP variants can be formed, as detailed in Table 4.

C Performance on Real-World Instances

Our test results on Real-World Instances datasets are presented in Tables 5, 6, and 7. All models are trained on instances of size $N = 100$. During inference, data augmentation is applied, and a greedy rollout strategy is adopted by default. Some results for comparative models are sourced from MVMoE [12] and RouteFinder [13].

D Licenses for Code and Datasets

The licenses for the codes and the datasets used in this work are listed in Table 8.

E Broader Impacts

This research contributes to the field of neural combinatorial optimization by employing advanced machine learning techniques to address large-scale and multi-variant VRP problems. We believe that the proposed multi-task knowledge distillation training framework, heavy decoder model, and Random Reordering Reconstruction (R3C) strategy can provide valuable insights and inspire subsequent work to explore more efficient and effective neural methods for solving large-scale and diverse VRP problems. As a general learning-based approach to solving the VRP, the proposed multi-task knowledge distillation training framework and R3C strategy do not inherently possess any specific potential negative social impacts.

Table 5: Results on small-scale CVRPLIB instances (Set-X) [25]. All models are trained on instances of size $N = 100$, and inference utilized data augmentation[8] and greedy rollout by default.

Set-X		POMO		POMO-MTL		MVMoE/4E		MVMOE/4E-L		MTL-KD	
Instance	Opt.	Obj.	Gap	Obj.	Gap	Obj.	Gap	Obj.	Gap	Obj.	Gap
X-n101-k25	27591	30138	9.231%	32482	17.727%	29361	6.415%	29015	5.161%	29058	5.317%
X-n106-k14	26362	39322	49.162%	27369	3.820%	27278	3.475%	27242	3.338%	26918	2.109%
X-n110-k13	14971	15223	1.683%	15151	1.202%	15089	0.788%	15196	1.503%	15407	2.912%
X-n115-k10	12747	16113	26.406%	14785	15.988%	13847	8.629%	13325	4.534%	13513	6.009%
X-n120-k6	13332	14085	5.648%	13931	4.493%	14089	5.678%	13833	3.758%	13657	2.438%
X-n125-k30	55539	58513	5.355%	60687	9.269%	58944	6.131%	58603	5.517%	57615	3.738%
X-n129-k18	28940	29246	1.057%	30332	4.810%	29802	2.979%	29457	1.786%	29309	1.275%
X-n134-k13	10916	11302	3.536%	11581	6.092%	11353	4.003%	11398	4.416%	11363	4.095%
X-n139-k10	13590	14035	3.274%	13911	2.362%	13825	1.729%	13800	1.545%	13911	2.362%
X-n143-k7	15700	16131	2.745%	16660	6.115%	16125	2.707%	16147	2.847%	15955	1.624%
X-n148-k46	43448	49328	13.533%	50782	16.880%	46758	7.618%	45599	4.951%	45463	4.638%
X-n153-k22	21220	32476	53.040%	26237	23.643%	23793	12.125%	23316	9.877%	23340	9.991%
X-n157-k13	16876	17660	4.646%	17510	3.757%	17650	4.586%	17410	3.164%	17161	1.689%
X-n162-k11	14138	14889	5.312%	14720	4.117%	14654	3.650%	14662	3.706%	14487	2.469%
X-n167-k10	20557	21822	6.154%	21399	4.096%	21340	3.809%	21275	3.493%	21053	2.413%
X-n172-k51	45607	49556	8.659%	56385	23.632%	51292	12.465%	49073	7.600%	47850	4.918%
X-n176-k26	47812	54197	13.354%	57637	20.549%	55520	16.121%	52727	10.280%	52476	9.755%
X-n181-k23	25569	37311	45.923%	26219	2.542%	26258	2.695%	26241	2.628%	25919	1.369%
X-n186-k15	24145	25222	4.461%	25000	3.541%	25182	4.295%	24836	2.862%	24711	2.344%
X-n190-k8	16980	18315	7.862%	18113	6.673%	18327	7.933%	18113	6.673%	17539	3.292%
X-n195-k51	44225	49158	11.154%	54090	22.306%	49984	13.022%	48185	8.954%	46301	4.694%
X-n200-k36	58578	64618	10.311%	61654	5.251%	61530	5.039%	61483	4.959%	60978	4.097%
X-n209-k16	30656	32212	5.076%	32011	4.420%	32033	4.492%	32055	4.564%	31536	2.871%
X-n219-k73	117595	133545	13.564%	119887	1.949%	121046	2.935%	120421	2.403%	118499	0.769%
X-n228-k23	25742	48689	89.142%	33091	28.549%	31054	20.636%	28561	10.951%	28156	9.378%
X-n237-k14	27042	29893	10.543%	28472	5.288%	28550	5.577%	28486	5.340%	27789	2.762%
X-n247-k50	37274	56167	50.687%	45065	20.902%	43673	17.167%	41800	12.143%	41106	10.281%
X-n251-k28	38684	40263	4.082%	40614	4.989%	41022	6.044%	40822	5.527%	39877	3.084%
Avg. Gap		16.629%		9.820%		6.884%		5.160%		4.025%	

Table 6: Results on VRPTW instances (Set-Solomon) [26]. All models are trained on instances of size $N = 100$, and inference utilized data augmentation[8] and greedy rollout by default.

Set-Solomon Instance	Opt.	POMO		POMO-MTL		MVMoE/4E		MVMOE/4E-L		MTL-KD	
		Obj.	Gap	Obj.	Gap	Obj.	Gap	Obj.	Gap	Obj.	Gap
R101	1637.7	1805.6	10.252%	1821.2	11.205%	1798.1	9.794%	1730.1	5.641%	1768.0	7.956%
R102	1466.6	1556.7	6.143%	1596.0	8.823%	1572.0	7.187%	1574.3	7.345%	1564.4	6.668%
R103	1208.7	1341.4	10.979%	1327.3	9.812%	1328.2	9.887%	1359.4	12.470%	1379.0	14.090%
R104	971.5	1118.6	15.142%	1120.7	15.358%	1124.8	15.780%	1098.8	13.100%	1074.1	10.561%
R105	1355.3	1506.4	11.149%	1514.6	11.754%	1479.4	9.157%	1456.0	7.433%	1465.2	8.109%
R106	1234.6	1365.2	10.578%	1380.5	11.818%	1362.4	10.352%	1353.5	9.627%	1346.1	9.031%
R107	1064.6	1214.2	14.052%	1209.3	13.592%	1182.1	11.037%	1196.5	12.391%	1193.9	12.145%
R108	932.1	1058.9	13.604%	1061.8	13.915%	1023.2	9.774%	1039.1	11.481%	1035.4	11.082%
R109	1146.9	1249.0	8.902%	1265.7	10.358%	1255.6	9.478%	1224.3	6.750%	1260.0	9.861%
R110	1068.0	1180.4	10.524%	1171.4	9.682%	1185.7	11.021%	1160.2	8.635%	1199.5	12.313%
R111	1048.7	1177.2	12.253%	1211.5	15.524%	1176.1	12.148%	1197.8	14.220%	1178.7	12.396%
R112	948.6	1063.1	12.070%	1057.0	11.427%	1045.2	10.183%	1044.2	10.082%	1057.2	11.448%
RC101	1619.8	2643.0	63.168%	1833.3	13.181%	1774.4	9.544%	1749.2	7.988%	1774.0	9.520%
RC102	1457.4	1534.8	5.311%	1546.1	6.086%	1544.5	5.976%	1556.1	6.771%	1588.4	8.989%
RC103	1258.0	1407.5	11.884%	1396.2	10.986%	1402.5	11.486%	1415.3	12.502%	1451.8	15.405%
RC104	1132.3	1261.8	11.437%	1271.7	12.311%	1265.4	11.755%	1264.2	11.649%	1241.6	9.653%
RC105	1513.7	1612.9	6.553%	1644.9	8.668%	1635.5	8.047%	1619.4	6.980%	1688.3	11.535%
RC106	1372.7	1539.3	12.137%	1552.8	13.120%	1505.0	9.638%	1509.5	9.968%	1468.8	7.001%
RC107	1207.8	1347.7	11.583%	1384.8	14.655%	1351.6	11.906%	1324.1	9.625%	1367.6	13.231%
RC108	1114.2	1305.5	17.169%	1274.4	14.378%	1254.2	12.565%	1247.2	11.939%	1232.3	10.600%
RC201	1261.8	2045.6	62.118%	1761.1	39.570%	1577.3	25.004%	1517.8	20.285%	1490.8	18.149%
RC202	1092.3	1805.1	65.257%	1486.2	36.062%	1616.5	47.990%	1480.3	35.520%	1336.5	22.356%
RC203	923.7	1470.4	59.186%	1360.4	47.277%	1473.5	59.521%	1479.6	60.182%	1237.8	34.005%
RC204	783.5	1323.9	68.973%	1331.7	69.968%	1286.6	64.212%	1232.8	57.342%	1066.0	36.056%
RC205	1154.0	1568.4	35.910%	1539.2	33.380%	1537.7	33.250%	1440.8	24.850%	1448.3	25.503%
RC206	1051.1	1707.5	62.449%	1472.6	40.101%	1468.9	39.749%	1394.5	32.671%	1354.7	28.884%
RC207	962.9	1567.2	62.758%	1375.7	42.870%	1442.0	49.756%	1346.4	39.831%	1235.9	28.352%
RC208	776.1	1505.4	93.970%	1185.6	52.764%	1107.4	42.688%	1167.5	50.437%	1064.0	37.096%
Avg. Gap		28.054%		21.380%		20.317%		18.490%		15.786%	

Table 7: Results on large-scale CVRPLIB instances (Set-X) [25]. All models are trained on instances of size $N = 100$, and inference utilized data augmentation[8] and greedy rollout by default.

Instance	Opt.	Set-X		POMO		LEHD		POMO-MTL		MVMoE/4E		MVMoE/4E-L		RF-MVMoE		RF-TE		MTL-KD	
		Obj.	Gap	Obj.	Gap	Obj.	Gap	Obj.	Gap	Obj.	Gap	Obj.	Gap	Obj.	Gap	Obj.	Gap	Obj.	Gap
X-n502-k39	69226	75617	9.232%	71438	3.195%	77284	11.640%	73533	6.222%	74429	7.516%	76338	10.274%	71791	3.705%	71124	2.742%		
X-n513-k21	24201	30518	26.102%	25624	5.880%	28510	17.805%	32102	32.647%	31231	29.048%	32639	34.866%	28465	17.619%	25947	7.215%		
X-n524-k153	154593	201877	30.586%	280556	81.480%	192249	24.358%	186540	20.665%	182392	17.982%	170999	16.612%	174381	12.800%	171305	10.811%		
X-n536-k96	94848	160673	11.837%	103785	9.425%	106514	12.302%	109581	15.536%	108543	14.441%	105847	11.599%	103272	8.884%	101893	7.430%		
X-n548-k50	86700	103093	18.908%	90644	4.549%	94562	9.068%	95894	10.604%	95917	10.631%	104289	20.287%	100956	16.443%	89169	2.848%		
X-n561-k42	42717	49370	15.575%	44728	4.708%	47846	12.007%	56008	31.114%	51810	21.287%	53383	24.969%	49454	15.771%	45467	6.438%		
X-n573-k30	50673	83545	64.871%	53482	5.543%	60913	20.208%	59473	17.366%	57042	12.569%	61524	21.414%	55952	10.418%	53466	5.512%		
X-n586-k159	190316	229887	20.792%	232867	22.358%	208893	9.761%	215668	13.321%	214577	12.748%	212151	11.473%	205575	8.018%	200863	5.542%		
X-n599-k92	108451	150572	38.839%	115377	6.386%	120333	10.956%	128949	18.901%	125279	15.517%	126578	16.714%	116560	7.477%	113513	4.668%		
X-n613-k62	59535	68451	14.976%	62484	4.953%	67984	14.192%	82586	38.718%	79495	25.884%	73456	23.383%	67267	12.987%	63035	5.879%		
X-n627-k43	62164	84434	35.825%	67568	8.693%	73060	17.528%	70987	14.193%	70905	14.061%	70414	13.271%	67572	8.700%	65755	5.777%		
X-n641-k35	63682	75573	18.672%	68249	7.172%	72643	14.071%	75329	18.289%	72655	14.090%	71975	13.023%	70831	11.226%	67593	6.141%		
X-n655-k131	106780	127211	19.134%	117532	10.069%	116988	9.560%	117678	10.206%	118475	10.952%	119057	11.497%	112202	5.078%	109748	2.780%		
X-n670-k130	146332	208079	42.197%	220927	50.977%	190118	29.922%	197695	35.100%	183447	25.364%	168226	14.962%	168999	15.490%	161076	10.076%		
X-n685-k75	68205	79482	16.534%	72946	6.951%	80892	18.601%	97388	42.787%	89441	31.136%	82269	20.620%	77847	14.137%	73249	7.395%		
X-n701-k44	81923	97843	19.433%	86327	5.376%	92075	12.392%	98469	20.197%	94924	15.870%	90189	10.090%	89932	9.776%	85967	4.936%		
X-n716-k35	43373	51381	18.463%	46502	7.214%	52709	21.525%	56773	30.895%	52305	20.593%	52250	20.467%	49669	14.516%	47012	8.390%		
X-n733-k159	136187	159098	16.823%	149115	9.493%	161961	18.925%	178322	30.939%	167477	22.976%	156387	14.833%	148463	9.014%	142712	4.791%		
X-n749-k98	77269	87788	13.611%	83439	7.985%	90582	17.229%	100438	29.985%	94497	22.296%	92147	19.255%	85171	10.227%	82295	6.505%		
X-n766-k71	114417	135464	18.395%	131487	14.919%	144041	25.891%	152352	33.155%	136255	19.086%	130505	14.061%	129935	13.563%	123310	7.772%		
X-n783-k48	72386	90289	24.733%	76766	6.051%	83169	14.897%	100383	38.677%	92960	28.423%	96336	33.087%	83185	14.919%	77332	6.833%		
X-n801-k40	73305	124278	69.536%	77546	5.785%	85077	16.059%	91560	24.903%	87662	19.585%	87118	18.843%	86164	17.542%	78041	6.460%		
X-n819-k71	185121	193451	22.344%	178558	12.925%	177157	12.039%	183599	16.113%	185832	17.525%	179596	13.581%	174441	10.321%	170672	7.938%		
X-n837-k142	193737	237884	22.787%	207709	7.212%	214207	10.566%	229526	18.473%	221286	14.220%	230362	18.904%	208528	7.635%	203165	4.866%		
X-n856-k95	88965	152528	71.447%	92936	4.464%	101774	14.398%	99129	11.425%	106816	20.065%	105801	18.924%	98291	10.483%	94079	5.748%		
X-n876-k59	99299	119764	20.609%	104183	4.918%	116617	17.440%	119619	20.463%	114333	15.140%	114016	14.821%	107416	8.174%	105873	6.620%		
X-n895-k37	53860	70245	30.421%	58028	7.739%	65587	21.773%	79018	46.710%	64310	19.402%	69099	28.294%	64871	20.444%	58606	8.812%		
X-n916-k207	329179	399372	21.324%	385208	17.021%	361719	9.885%	383681	16.557%	374016	13.621%	373600	13.494%	352998	7.236%	346940	5.396%		
X-n936-k151	132715	237625	79.049%	196547	48.097%	186262	40.347%	220926	66.466%	190407	43.471%	161343	21.571%	163162	22.942%	152094	14.602%		
X-n957-k87	85465	130850	53.104%	90295	5.651%	98198	14.898%	113882	33.250%	105629	23.593%	123633	44.659%	102680	20.153%	90407	5.782%		
X-n979-k58	118976	147687	24.132%	127972	7.561%	138092	16.067%	146347	23.005%	139682	17.404%	131754	10.740%	129952	9.225%	127650	7.291%		
X-n1001-k43	72355	100399	38.759%	76689	5.990%	87660	21.153%	114448	58.176%	94734	30.929%	88969	22.962%	85929	18.760%	78833	8.953%		
Avg. Gap		29.658%	12.836%	16.796%	26.408%	19.607%	18.795%	18.795%	12.303%	6.655%									

Table 8: Licenses of Used Codes and Datasets

Type	Resource	License Type	URL / Reference
Code	MVMoE[12]	MIT License	https://github.com/RoyalSkye/Routing-MVMoE
Code	MT-POMO[11]	MIT License	https://github.com/FeiLiu36/MTNCO
Code	HGS-PyVRP[24]	MIT License	https://github.com/PyVRP/PyVRP
Code	OR-Tools[6]	Apache License	https://github.com/google/or-tools
Dataset	CVRPLIB(Set-X)[25]	Available for academic research use	http://vrp.galgos.inf.puc-rio.br/index.php/en/
Dataset	Solomon[26]	Available for academic research use	https://www.sintef.no/projectweb/top/vrptw/solomon-benchmark/